Available online at www.sciencedirect.com
ScienceDirect
Journal of Solid State Chemistry 181 (2008) 1103–1109
JOURNAL OF SOLID STATE CHEMISTRY
www.elsevier.com/locate/jssc

Supramolecular open-framework based on 1-D iron phosphate–diphosphate chains assembled through hydrogen bonding

Miguel A. Salvadó, Pilar Pertierra, Camino Trobajo, José R. García*

Departamentos de Química Física y Analítica y Química Orgánica e Inorgánica, Universidad de Oviedo, 33006 Oviedo, Spain

Received 9 November 2007; received in revised form 22 January 2008; accepted 5 February 2008
Available online 26 February 2008

Abstract

$Fe(H_2PO_4)(H_2P_2O_7)\cdot C_5H_5N$, a new iron(III) phosphate with an open-framework has been synthesized hydrothermally using pyridine as organic template. The crystal structure was solved *ab initio* using conventional powder X-ray diffraction data. The unit cell is orthorhombic, $a = 9.5075(2)$, $b = 10.1079(1)$, $c = 13.3195(2)$ Å, space group $P2_12_12_1$, $Z = 4$. The structure consists of FeO_6 octahedra joined by H_2PO_4 and $H_2P_2O_7$ groups forming linear chains interconnected by hydrogen bonding to give rise to a supramolecular framework enclosing tunnels in which the pyridine molecules reside.

Keywords: Hydrothermal synthesis; Iron phosphates; Open frameworks

1. Introduction

The inorganic materials with open-framework are of great interest in material science because of their potential applications in many fields such as catalysis, ion exchange, adsorption or separation [1,2]. Within these compounds transition metal phosphates composes an important class. In the mineral kingdom, iron phosphates are among the most important materials besides silicates and aluminates. The most striking example of an open-framework iron–phosphate is provided by the mineral cacoxenite which contains cylindrical tunnels occupied by water molecules, with a free diameter of 14.2 Å. In the last years, a number of iron phosphates and fluorophosphates haven been reported [3–20]. Many of them were synthesized by using hydrothermal methods and organic templates. In addition to their use as structure-directing agents in the solvothermal synthesis of three-dimensional zeolite and zeotype frameworks, organic amines have now been employed in the preparation of several low dimensional metal phosphates. Thus, iron phosphates with two-dimensional [10–16], and one-dimensional (1-D) architectures [8,9,17–20] have been synthesized and characterized. The stabilization of layered and chain-like arrangements usually requires specific conditions [21]. The compounds can contain cations located between the sheets or chains, separating negative moieties and introducing a favorable term in the energy of the system. Protonation reduces the overall charge on the layers or chains and allows the formation of stabilizing hydrogen bonds across the van der Waals gap. In addition, layered and chain compounds also have fascinating chemical reactivity, leading themselves to intercalation–deintercalation processes, pillaring reactions, and acid–base chemistry involving a condensation of parts of the framework to obtain related, but new, structures.

Two parameters relative to the nature of the amine are important: the size and shape of the amine and its correlated ability to be protonated [22]. Generally aliphatic diamines are used as templates giving rise to frameworks negatively charged with the amine protonated. The presence of strong electrostatic interactions with the framework determines the final structure and makes difficult extraction of the template after the synthesis. Pyridine has been very little used as template. It has two characteristics that differentiate from other small templates: it has only a nitrogen atom with a low basicity and it has a planar geometry.

*Corresponding author. Fax: +34 985103446.
E-mail address: jrgm@uniovi.es (J.R. García).

0022-4596/$ - see front matter © 2008 Elsevier Inc. All rights reserved.
doi:10.1016/j.jssc.2008.02.012

This paper describes the synthesis and structure of a new iron(III) phosphate where pyridine is used as template and where the obtained 1-D framework is stabilised by hydrogen bonds.

2. Experimental

2.1. Synthesis

$Fe(H_2PO_4)(H_2P_2O_7)\cdot C_5H_5N$ was performed under hydrothermal conditions in a stainless steel Teflon-lined vessel, under autogenous pressure, in the presence of pyridine by mixing 85% H_3PO_4 and 1 M $FeCl_3\cdot 6H_2O$ in a molar ratio 1:10:10:66 ($FeCl_3$:H_3PO_4:C_5H_5N:H_2O) with a total volume of 40 cm^3 and heating for 6 days at 180 °C. $Fe(H_2PO_4)(H_2P_2O_7)\cdot 5H_2O$ was prepared by successive treatment of $Fe(H_2PO_4)(H_2P_2O_7)\cdot C_5H_5N$ with 0.1 M HCl solution while stirring (V/m ratio 100:1, cm^3/g) for three times, 4 h each, up to total removal of the amine. In both cases, the obtained solids were filtered, washed with distilled water, and dried at room temperature.

2.2. Analytical procedures

The phosphorus and iron contents of the solids was determined with a SpectraSpectrometer DCP-AEC after dissolving a weighted amount of sample in $HF_{(aq)}$. Microanalytical data (C, N and H) were obtained with a Perkin–Elmer model 2400B. Elemental analysis (wt%) for $Fe(H_2PO_4)(H_2P_2O_7)\cdot C_5H_5N$: Fe 13.1(3), P 22.4(4), N 3.5(1), C 14.8(2), H 2.0(3) (calcd. Fe 13.68, P 22.80, N 3.43, C 14.71, H 2.21). Elemental analysis (wt%) for $Fe(H_2PO_4)(H_2P_2O_7)\cdot 5H_2O$: Fe 12.9(4), P 21.8(5), N 0.2(1), C 0.6(1), H 2.9(3) (calc. Fe 13.33, P 22.18, H 3.37). Thermogravimetric analysis was obtained under air atmosphere with a Mettler TA4000-TG50 thermoanalyzer at a heating rate of 10 °C min^{-1}. Infra-red spectra were recorded with a Perkin–Elmer 1000 FT-IR spectrophotometer. Electron micrographs were recorded with a JEOL JSM 6100 electron microscope operating a 20 kV.

2.3. X-ray crystallographic analysis

A powder pattern of $Fe(H_2PO_4)(H_2P_2O_7)\cdot C_5H_5N$ was collected on a Seifert XRD3000 high resolution powder X-ray diffractometer belonging to the SCT's facilities of the University of Oviedo operating in Bragg–Brentano θ–θ geometry at 50 kV and 40 mA using graphite monochromated Cu$K\alpha$ radiation. The sample was gently ground in an agate mortar and mixed with Cab-osil® in order to minimize the preferred orientation effects. Data was collected at room temperature over the angular 2θ range 9–110° with a step size of 0.01° and a count time of 10 s/step. The pattern was indexed in the orthorhombic system using the program TREOR [23] ($M_{20}=22$, $F_{20}=38$ (0.010, 52)). Intensities were extracted with the LeBail method and the program FULLPROF [24]. The structure was solved by direct methods and Fourier recycling with the program EXPO [25] in the space group *Pnma*. Refinement of the structure was carried out by the Rietveld method and the GSAS package [26] in *Pnma* but the refinement did not progress adequately. Furthermore the pyridine molecule was located perpendicular to a symmetry plane not compatible with its point group symmetry. Then the refinement was carried out in two maximal subgroups: $Pn2_1a$ and $P2_12_12_1$. The refinement progressed well in the last one with good final agreement *R*-factors and minimal profile differences. The structure was refined with soft constraints for Fe–O and P–O bond distances as well as for pyridine molecule geometry. A preferred orientation correction was introduced through the spherical harmonic (ODF) model [27] using six coefficients resulting in a texture index of 1.51. The first peak, being severely affected by preferred orientation was excluded from the Rietveld refinement. The final Rietveld plot is shown in Fig. 1. The crystallographic parameters are presented in Table 1. Final atomic coordinates, selected bond distances, and intermolecular contacts are reported in Tables 2 and 3.

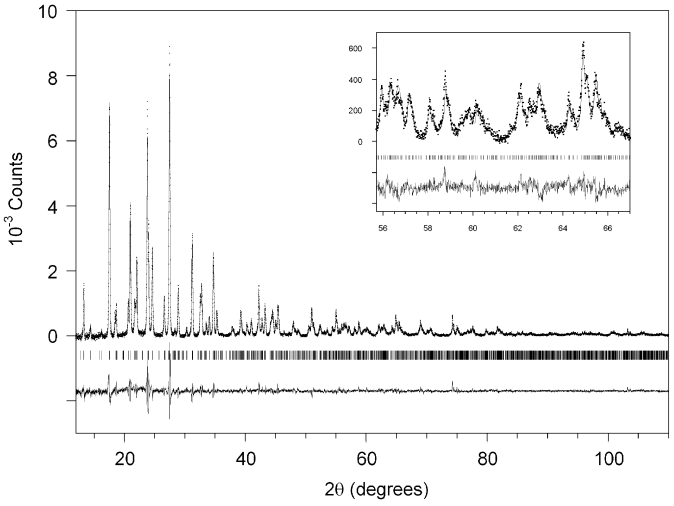

Fig. 1. Powder X-ray diffraction pattern of $Fe(H_2PO_4)(H_2P_2O_7)\cdot C_5H_5N$. Observed (points), calculated (continuous line) and difference (below) profiles are plotted on the same scale. Bragg peaks are indicated by tick marks. Background has been subtracted for more clarity.

3. Results and discussion

$Fe(H_2PO_4)(H_2P_2O_7)\cdot C_5H_5N$ is constituted by polycrystalline aggregates of fibrous morphology (Fig. 2a). The presence of diphosphate groups was confirmed by IR data (Fig. 3a). Although the characteristic signal of the ν_{as}(P–O–P) vibration (ca. 950 cm^{-1}) are less resolved due to the coexistence of PO_4 and P_2O_7 groups, the band at 745 cm^{-1} can be assigned unambiguously to the ν_s(P–O–P) vibration [28,29]. The structure of the title compound is formed by inorganic chains interconnected by hydrogen bonds forming channels in the direction [100]. Inside these channels are located the pyridine molecules (Fig. 4). The chains are thus held together by a network of hydrogen

Table 1
Crystal data and structure refinement for $Fe(H_2PO_4)(H_2P_2O_7)\cdot C_5H_5N$

Empirical formula	$FeP_3O_{11}C_5NH_9$
Formula weight	407.89
Crystal system	Orthorhombic
Unit cell dimensions	$a = 9.5075(2)$ Å
	$b = 10.1079(1)$ Å
	$c = 13.3195(2)$ Å
Volume	1280.02(4) Å^3
Z	4
Density (calculated)	2.117 Mg/m^3
2θ range	12–110°
Step	0.01°
Observed reflections	1903
Parameters	103
R_{wp}	6.9
R_{exp}	4.0
χ^2	3.0
$R(F^2)$	8.5

Table 2
Fractional atomic coordinates and isotropic displacement parameters (Å^2) for $Fe(H_2PO_4)(H_2P_2O_7)\cdot C_5H_5N$

Atom	x	y	z	B
Fe	0.6090(3)	0.2493(8)	0.4819(2)	0.87(4)
P1	0.8797(4)	0.1103(3)	0.3785(3)	0.80(4)
P2	0.1255(4)	0.8901(3)	0.1220(3)	0.80(4)
P3	0.3458(5)	0.254(1)	0.3230(3)	0.80(4)
O1	0.7345(6)	0.1019(8)	0.4238(7)	1.37(6)
O2	0.0003(7)	0.1133(9)	0.4527(5)	1.37(6)
O3	0.0170(7)	0.8955(8)	0.0388(5)	1.37(6)
O4	0.2697(6)	0.8915(8)	0.0747(6)	1.37(6)
O5	0.4938(9)	0.225(1)	0.3586(7)	1.37(6)
O6	0.7274(9)	0.228(1)	0.6070(6)	1.37(6)
O7	0.393(1)	0.2498(4)	0.6745(4)	1.37(6)
O8	0.890(2)	0.0081(6)	0.2944(5)	1.37(6)
O9	0.095(1)	0.9966(6)	0.2004(5)	1.37(6)
O10	0.325(1)	0.1515(6)	0.2364(8)	1.37(6)
O11	0.663(1)	0.8954(7)	0.2294(7)	1.37(6)
N1	0.7626(1)	0.1213(2)	0.07988(8)	1.4(2)
C2	0.6710(1)	0.1873(4)	0.14563(9)	1.4(2)
C3	0.3296(1)	0.8157(4)	0.35734(8)	1.4(2)
C4	0.2392(1)	0.8930(2)	0.42121(8)	1.4(2)
C5	0.1598(1)	0.8341(4)	0.4883(1)	1.4(2)
C6	0.8405(2)	0.1914(4)	0.0129(1)	1.4(2)

Table 3
Selected bond distances, intermolecular contacts (Å) and bond-valence sums ($\sum$s) for $Fe(H_2PO_4)(H_2P_2O_7)\cdot C_5H_5N$

P1–O1	1.509(7)	P2–O3	1.515(7)	P3–O5	1.51(1)
P1–O2	1.514(7)	P2–O4	1.509(7)	P3–O6	1.47(1)
P1–O7	1.586(6)	P2–O7	1.587(6)	P3–O10	1.56(1)
P1–O8	1.528(7)	P2–O9	1.528(7)	P3–O11	1.59(1)
$\sum$s(P1–O)	5.019	$\sum$s(P2–O)	5.012	$\sum$s(P3–O)	5.017
Fe–O1	2.059(9)	O8···O9	2.32(2)	N1···O1	3.068(8)
Fe–O2	1.94(1)	O8···O11	2.59(2)	N1···O8	3.306(8)
Fe–O3	2.04(1)	O9···O10	2.73(2)	N1···O11	3.174(9)
Fe–O4	1.991(9)				
Fe–O5	1.99(1)				
Fe–O6	2.023(9)				
$\sum$s(Fe–O)	3.090				

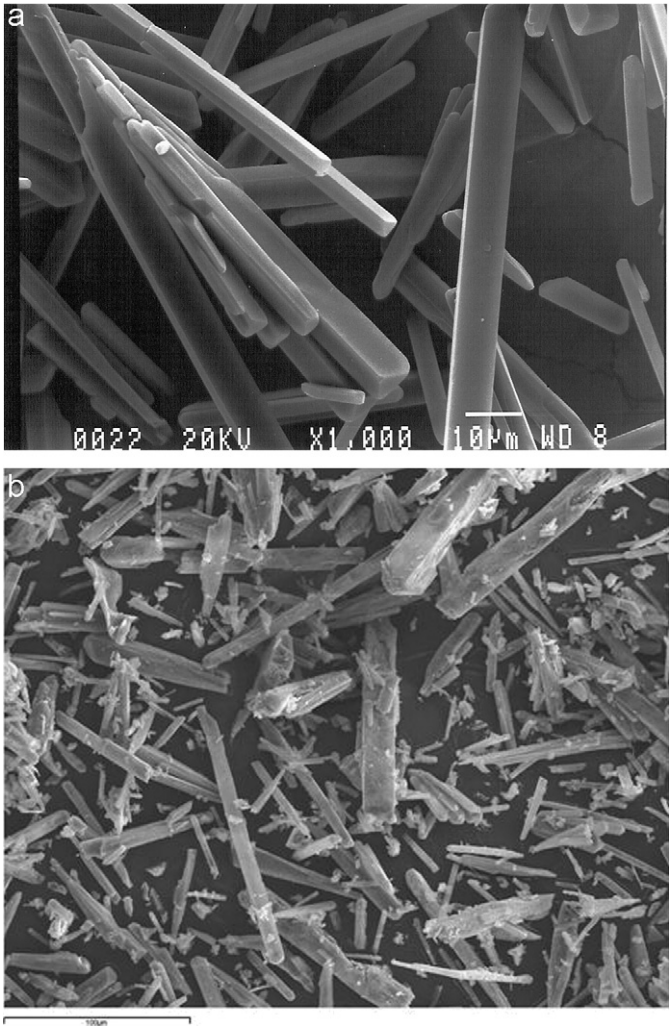

Fig. 2. SEM images of: (a) $Fe(H_2PO_4)(H_2P_2O_7)\cdot C_5H_5N$ and (b) $Fe(H_2PO_4)(H_2P_2O_7)\cdot 5H_2O$.

bonds involving only interchain interactions (Fig. 5). In the inorganic chains, FeO_6 octahedra is joined through a dihydrogenphosphate and a dihydrogendiphosphate bridge where this last group is joined to each Fe atom by two O atoms. The four phosphate–diphosphate terminal oxygens are involved in strong interchain hydrogen bonds with an average O···O contact distance of 2.55 Å, all of them with other terminal oxygen atoms. The chains are thus held together by a network of hydrogen bonds involving only interchain interactions. An OH group, belonging to the dihydrogenphosphate group, as well as acceptor of an interchain hydrogen bond also forms probably a hydrogen bond acting as donor with the nitrogen atom of the pyridine (O11···N1, 3.17 Å). The geometry of this contact (e.g. angle C2–N1···O11 is 76°, far from 120°) and the absence of other contacts with ideal angle value suggest that the pyridine molecule is not protonated and acts as an

acceptor instead of a donor of a hydrogen bond. In any case, the pyridine with his unique basic center is not capable to link two chains and the structure indicates that it is merely occupying the void space formed by the supramolecular aggregation of four metal phosphate chains. Bond valence sum calculations [30], listed in Table 3, are in good agreement with the formal oxidation states of all atoms.

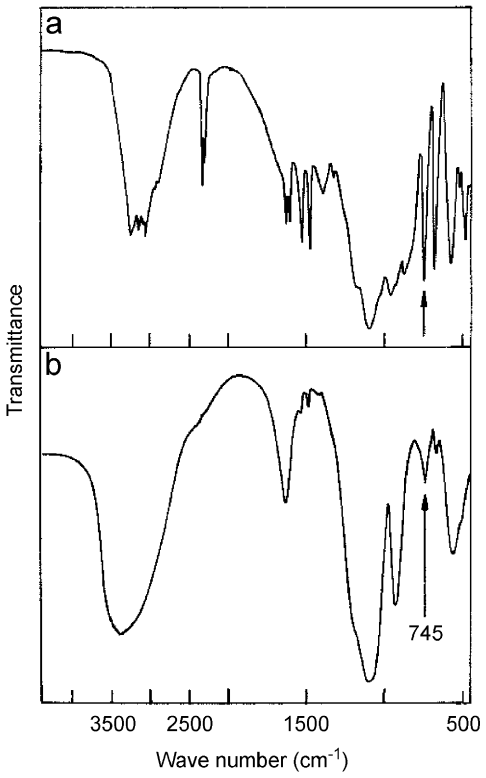

Fig. 3. FTIR spectra of: (a) $Fe(H_2PO_4)(H_2P_2O_7)\cdot C_5H_5N$ and (b) $Fe(H_2PO_4)(H_2P_2O_7)\cdot 5H_2O$.

$Fe(H_2PO_4)(H_2P_2O_7)\cdot C_5H_5N$ is stable up to 250 °C. From this temperature a total weight of 29.0% is lost (calcd. 28.20%) corresponding to one pyridine molecule and two water molecules. The TG-curve (Fig. 6a) shows the release of the amine in two consecutive steps, first approximately between 250 and 440 °C a 75% of the total amine content left the material, the rest is desorbed between 440 and 560 °C. Simultaneously to the amine desorbing is possible that condensation of hydroxyl groups occurs at a limited extent. This reaction is activated when the channels become empty and the structure is destabilized. In a first stage the zones close to the crystallite surface condense firstly. The formation of the condensed phase (metaphosphate, much dense) in the external zones of the crystal make difficult the diffusion of water molecules being trapped inside the material, now polyphasic, and this will be reflected in a complicated and not easily reproducible TG-curve (above 560 °C) due to the fact that the decomposition process is controlled now by complex diffusion mechanisms. The final product obtained at 900 °C was characterized by powder X-ray diffraction (Fig. 7) and identified as $Fe(PO_3)_3$ [31].

The 1-D organically templated iron phosphates are relatively scarce [8,9,17–20]. In most of them, the structures consist of $[FeX(HPO_4)_2]^{2-}_n$ (X=OH, F) chains of the

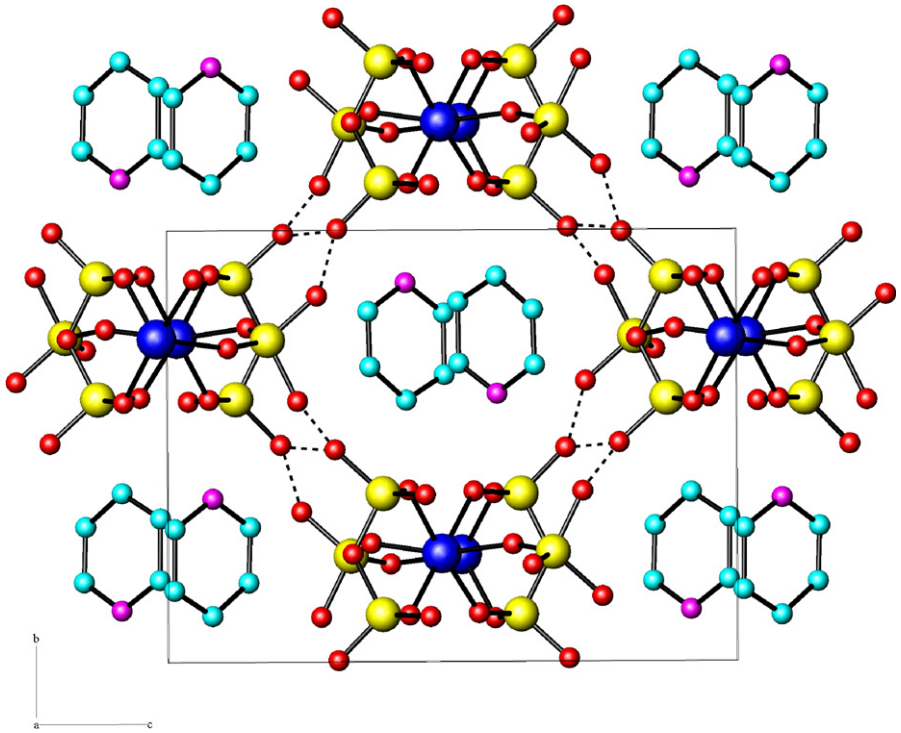

Fig. 4. View along the *a* axis showing the arrangement of the 1-D phosphate chains and the pyridine molecules. Metal (iron), phosphorus, oxygen, carbon and nitrogen are represented in blue, yellow, red, light blue and purple, respectively. Dashed lines indicate hydrogen bond contacts.

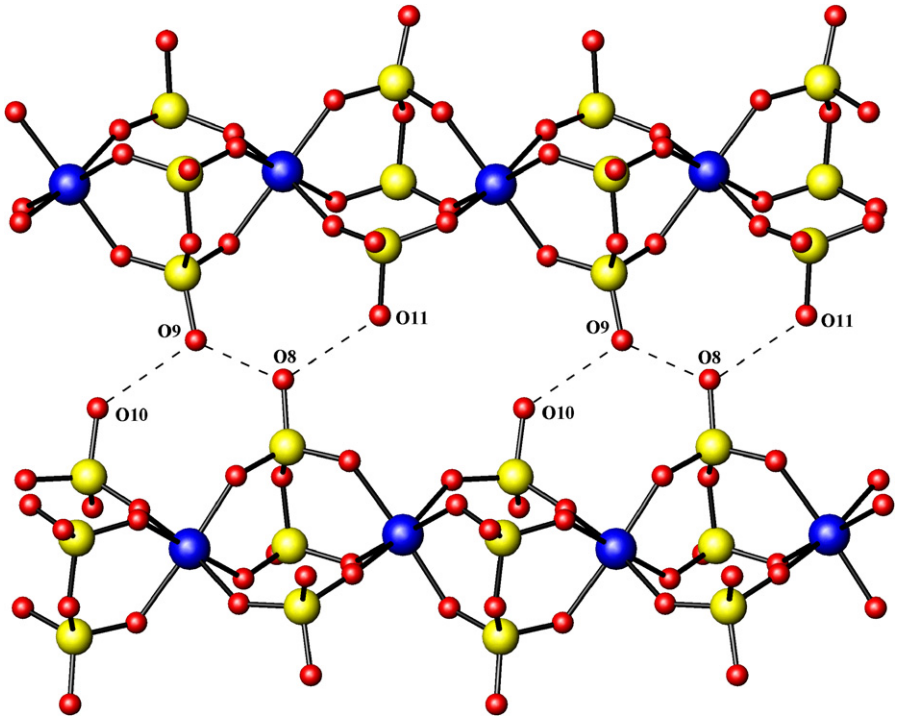

Fig. 5. A fragment of two adjacent inorganic chains (color code as Fig. 4).

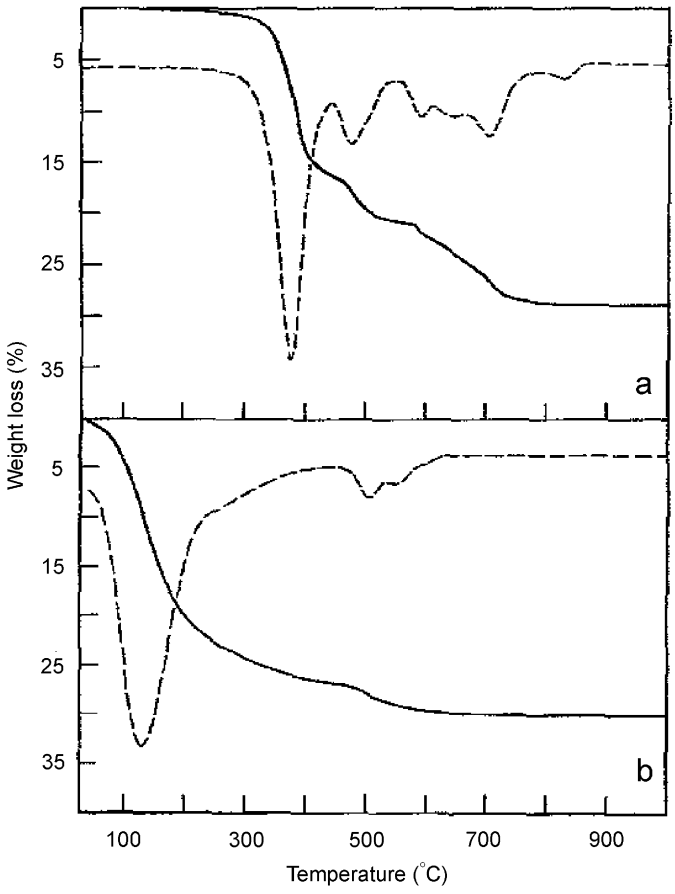

Fig. 6. TG (–) and DTG (- - -) curves of: (a) $Fe(H_2PO_4)(H_2P_2O_7)\cdot C_5H_5N$ and (b) $Fe(H_2PO_4)(H_2P_2O_7)\cdot 5H_2O$.

tancoite type, with the diprotonated amines inserted in between. In another one case, the infinite chain is constructed from phosphate groups and tetranuclear iron–oxygen clusters. In all, the 1-D chains are constituted both by Fe–O–P–O–Fe and Fe–O–Fe (or Fe–F–Fe) paths and are negatively charged with the charge balanced by a protonated amine. For the compound described here only Fe–O–P–O–Fe paths are present and the 1-D chains are neutral, with the structure being held by hydrogen bonds between neighbor chains and the pyridine molecules merely filling the channels formed in the structure.

Up to the best of our knowledge this is the first time this type of monodimensional chain is described in iron phosphate. A similar chain has been previously described in both gallium and vanadium phosphates synthesized in the presence of ethylenediamine, $[NH_3CH_2CH_2NH_3][M(H_2PO_4)(P_2O_7)]$ (M = V, Ga) [32]. The difference between the two chains are in the coordination of phosphate–diphosphate groups around metal atom. In our compound, phosphate groups are in *trans* position with the diphosphate groups occupying the equatorial plane while in V- and Ga-compounds the phosphate groups are in *cis* position (Fig. 8). Furthermore the structure is completed with doubly protonated diamine cations. In this case, the chains are held together by a network of hydrogen bonds involving both interchain and chain-diamine interactions and no channels are formed into the framework. A third type of metal–phosphate chain found previously in a Zn-compound can be also related with the former compounds. The structure of $Zn(H_2PO_4)_2$

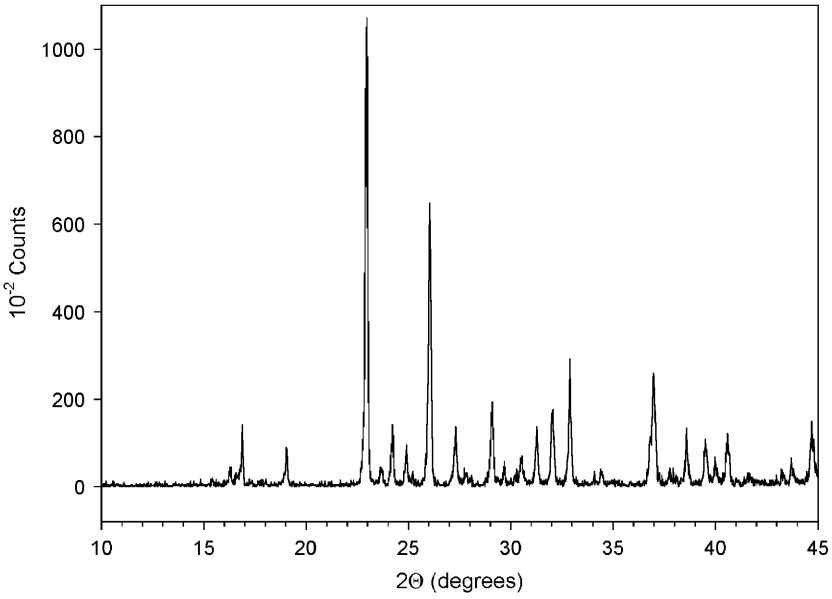

Fig. 7. Powder X-ray diffraction pattern of $Fe(H_2PO_4)(H_2P_2O_7)\cdot C_5H_5N$ treated at 900 °C.

$(HPO_4)\cdot H_2N_2C_6H_{12}$ has the same space group as the title compound and cell parameters are comparable although several important differences are remarkable [33]: Zn is four coordinated, no P–O–P bonds are present and the chains are interconnected through the doubly protonated dabconium cations by hydrogen bonding. The diphosphate group in both Fe and Ga (and V) compounds is "hydrolyzed" in Zn compound and the separation of the two phosphate groups implies the lost of two bonds with the metal which is well suited to the tetracoordinated Zn(II). Apart from the organic molecules, Zn structure are the logical counterparts of former compounds when changing from six to four metal coordination.

The determined structure predicts that pyridine molecules are loosely held in the channels in the absence of electrostatic or hydrogen bond interactions with the framework. In fact, when the sample was treated with 0.1 M HCl, elemental analysis (see Section 2.2) and both infrared (Fig. 3b) and thermogravimetric data (Fig. 6b) showed that the resulting solid was pyridine free and replaced by approximately five water molecules. $Fe(H_2PO_4)(H_2P_2O_7)\cdot 5H_2O$ dehydrates in a wide range from room temperature to nearly 300 °C. The amplitude of the DTG band indicates probably that the process occurs in several overlapping stages. When the channels become empty the process of condensation begins, being completed about 650 °C. The total weight lost up to 900 °C is 29.6% (calcd. 30.09%). Unfortunately, the hydrated compound has a disordered structure that prevents their solution from X-ray diffraction data. Nevertheless the SEM micrographs (Fig. 2b) show that the fibrous morphology was kept, indicating that 1-D phosphate chains are preserved as it can be expected of such soft treatment. The destruction of long range order between chains can be explained by a disordered substitution of interchain hydrogen bonds by water-chain hydrogen bonds.

One relevant feature in the title compound structure is the presence of $H_2P_2O_7$ groups acting as double bridges between two metal atoms. The P–O bonds of the P1–O7–P2 bridge are substantially longer (P1–O7, 1.586(6) Å and P2–O7, 1.587(6) Å) than terminal P–O bonds. The P–O–P angle experimentally determined is 126.1(4)° in accordance with the relationship between P–O bridging bond lengths and P–O–P bridging angles in P_2O_7 units observed previously in a number of diphosphate structures: P–O bridging bond lengths in the range 1.63–1.54 Å typically have P–O–P angles in the range 123–180° [34]. This type of union is rather unusual in metal phosphates frameworks synthesized under hydrothermal conditions with an organic template. Condensation of phosphate groups are generally observed in synthesis at temperatures above 500 °C and the compounds obtained are habitually formed exclusively by condensed phosphate anions. A remarkably feature of the title compound is the simultaneous presence of both mono- and diphosphate groups in an open structure of what only a few examples are known [35–37]. This offers new possibilities of metal phosphates with mixed octahedral–tetrahedral open-frameworks possessing not only monophosphate but also diphosphate or other condensed groups as building blocks.

Acknowledgments

We thank financial support from Spanish Ministerio de Educación y Ciencia (MAT2006-13548-C02-02, MAT2006-01997 and Factoría de Cristalización – Consolider Ingenio 2010) and Gobierno del Principado de Asturias (PCTI 2006-2009).

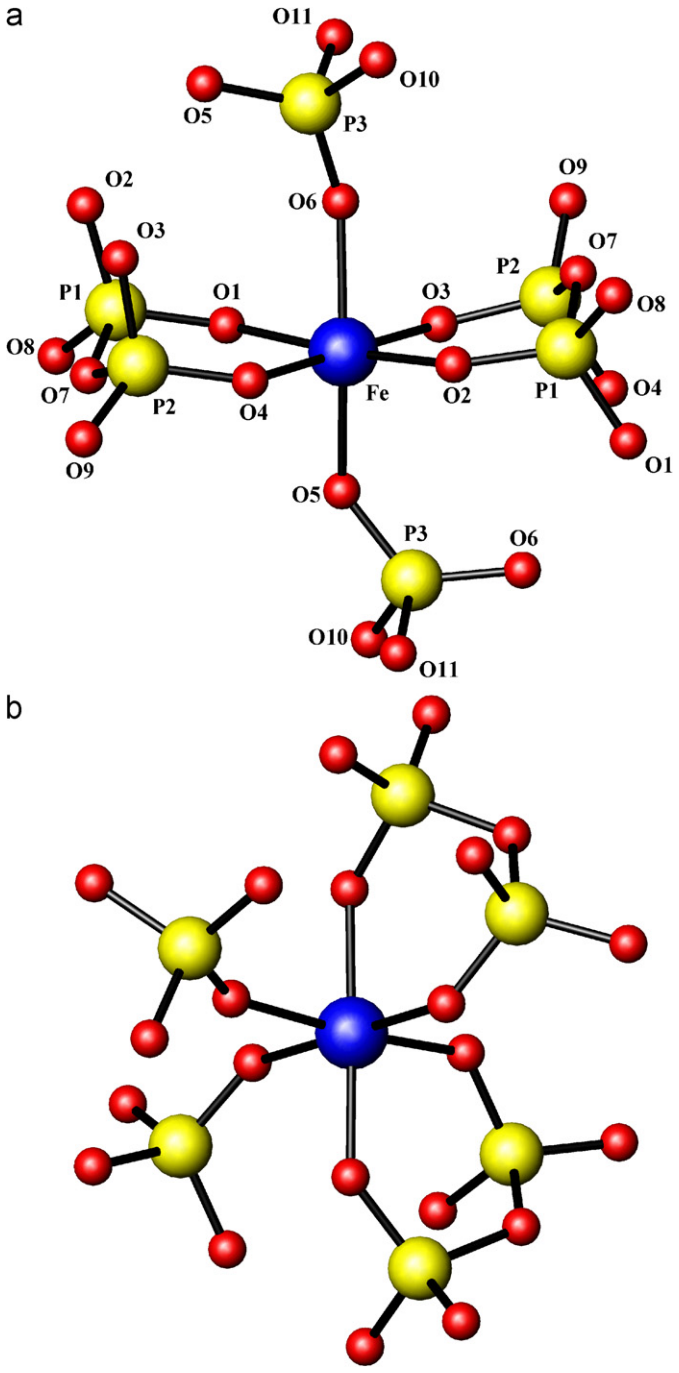

Fig. 8. Local coordination around metal atoms (color code as Fig. 4): (a) $Fe(H_2PO_4)(H_2P_2O_7)\cdot C_5H_5N$ and (b) $[NH_3CH_2CH_2NH_3]Ga(H_2PO_4)(H_2P_2O_7)$.

References

[1] K. Cheetham, G. Férey, T. Loiseau, Angew. Chem. Int. Ed. 38 (1999) 3268.

[2] S. Natarajan, S. Mandal, P. Mahata, V.K. Rao, P. Ramaswamy, A. Banerjee, A.K. Paul, K.V. Ramya, J. Chem. Sci. 118 (2006) 525.

[3] K.-H. Lii, Y.-F. Huang, V. Zima, C.-Y. Huang, H.-M. Lin, Y.-C. Jiang, F.-L. Liao, S.-L. Wang, Chem. Mater. 10 (1998) 2599 (and references therein).

[4] M.B. Korzenski, G.L. Schimek, J.W. Kolis, Eur. J. Solid State Inorg. Chem. 35 (1998) 143.

[5] K.-H. Lii, Y.-F. Huang, Chem. Commun. (1997) 839.

[6] M.A. Salvadó, P. Pertierra, S. García-Granda, A. Espina, C. Trobajo, J.R. García, Inorg. Chem. 38 (1999) 5944.

[7] K.-H. Lii, Y.-F. Huang, J. Chem. Soc. Dalton Trans. (1997) 2221.

[8] S. Mandal, M.A. Green, S. Natarajan, J. Solid State Chem. 177 (2004) 1117.

[9] S. Mahesh, M.A. Green, S. Natarajan, J. Solid State Chem. 165 (2002) 334.

[10] V. Zima, K.-H. Lii, N. Nguyen, A. Ducouret, Chem. Mater. 10 (1998) 1914.

[11] M. Cavellec, D. Riou, G. Ferey, Acta Cryst. C 51 (1995) 2242.

[12] J.R.D. DeBord, W.M. Reiff, R.C. Haushalter, J. Zubieta, J. Solid State Chem. 125 (1996) 186.

[13] R. Cowley, A.M. Chippindale, J. Chem. Soc. Dalton Trans. (2000) 3425.

[14] K.-H. Lii, Y.-F. Huang, Chem. Commun. (1997) 1311.

[15] S. Mandal, S. Natarajan, J.M. Grenèche, M. Riou-Cavellec, G. Férey, Chem. Mater. 14 (2002) 3751.

[16] A. Mgaidi, H. Boughzala, A. Driss, R. Clerac, C. Coulon, J. Solid State Chem. 144 (1999) 163.

[17] Z.A.D. Lethbridge, P. Lightfoot, R.E. Morris, D.S. Wragg, P.A. Wright, A. Kvick, G. Vaughan, J. Solid State Chem. 142 (1999) 455.

[18] V. Zima, K.-H. Lii, J. Chem. Soc. Dalton Trans. (1998) 4109.

[19] M. Cavellec, D. Riou, J.M. Grenéche, G. Férey, Inorg. Chem. 36 (1997) 2187.

[20] S. Mandal, S. Natarajan, W. Klein, M. Panthöfer, M. Jansen, J. Solid State Chem. 173 (2003) 367.

[21] J. Rouxel, Acc. Chem. Res. 25 (1992) 328.

[22] G. Férey, Chem. Mater. 13 (2001) 3084.

[23] P.E. Werner, L. Eriksson, M. Westdahl, J. Appl. Crystallogr. 18 (1985) 367.

[24] J. Rodríguez-Carvajal, in: Collected Abstracts of Powder Diffraction Meetings, Toulouse, France, 1990, p. 127.

[25] A. Altomare, M.C. Burla, G. Cascarano, G. Giacovazzo, A. Guagliardi, A.G.G. Moliterni, G. Polidori, J. Appl. Cryst. 28 (1995) 842.

[26] A.C. Larson, R.B. Von Dreele, General structure analysis system (GSAS), Los Alamos National Laboratory Report LAUR, 1994, p. 86.

[27] R.B. Von Dreele, J. Appl. Cryst. 30 (1997) 517.

[28] P. Bénard, V. Brandel, N. Dacheux, S. Jaulmes, S. Launay, C. Lindecker, M. Genet, D. Louër, M. Quarton, Chem. Mater. 8 (1996) 181.

[29] N. Dacheux, N. Clavier, G. Wallez, V. Brandel, J. Emery, M. Quarton, M. Genet, Mater. Res. Bull. 40 (2005) 2225.

[30] I.D. Brown, D. Altermatt, Acta Cryst. B 41 (1985) 244.

[31] $Fe(PO_3)_3$, file number 44-772, Joint Committee on Powder Diffraction Data Standards, International Center of Diffraction Data, Swarthmore, PA.

[32] A.M. Chippindale, Chem. Mater. 12 (2000) 818.

[33] J. Patarin, B. Marler, L. Huve, Eur. J. Solid State Inorg. Chem. 31 (1994) 909.

[34] N.S. Mandel, Acta Cryst. B 31 (1975) 1730.

[35] V. Ogorodnyk, I.V. Zatovsky, N.S. Slobodyanik, V.N. Baumer, O.V. Shishkin, J. Solid State Chem. 179 (2006) 3681.

[36] C. Falah, H. Boughzala, T. Jouini, A. Madani, J. Solid State Chem. 173 (2003) 342.

[37] A. Leclaire, B. Raveau, Mater. Res. Bull. 41 (2006) 967.